# The Light Peak of the Electroretinogram Is Dependent on Voltage-gated Calcium Channels and Antagonized by Bestrophin (Best-1)

Lihua Y. Marmorstein,[1] Jiang Wu,[3] Precious McLaughlin,[1] John Yocom,[1] Mike O. Karl,[4] Rudgar Neussert,[4] Soenke Wimmers,[4] J. Brett Stanton,[1] Ronald G. Gregg,[5] Olaf Strauss,[4] Neal S. Peachey,[3,6] and Alan D. Marmorstein[1,2]

[1]Department of Ophthalmology and Vision Science and [2]Optical Sciences Center, University of Arizona, Tucson, AZ 85711
[3]Cole Eye Institute, Cleveland Clinic Foundation, Cleveland, OH 44195
[4]Experimentelle Ophthalmologie Universitaetsklinkum Hamburg-Eppendorf, Hamburg, Germany
[5]Biochemistry and Molecular Biology, Ophthalmology and Visual Science, University of Louisville, KY 40202
[6]Research Service, Cleveland VA Medical Center, Cleveland, OH 44106

Mutations in *VMD2*, encoding bestrophin (best-1), cause Best vitelliform macular dystrophy (BMD), adult-onset vitelliform macular dystrophy (AVMD), and autosomal dominant vitreoretinochoroidopathy (ADVIRC). BMD is distinguished from AVMD by a diminished electrooculogram light peak (LP) in the absence of changes in the flash electroretinogram. Although the LP is thought to be generated by best-1, we find enhanced LP luminance responsiveness with normal amplitude in $Vmd2^{-/-}$ mice and no differences in cellular $Cl^-$ currents in comparison to $Vmd2^{+/+}$ littermates. The putative $Ca^{2+}$ sensitivity of best-1, and our recent observation that best-1 alters the kinetics of voltage-dependent $Ca^{2+}$ channels (VDCC), led us to examine the role of VDCCs in the LP. Nimodipine diminished the LP, leading us to survey VDCC β-subunit mutant mice. *Lethargic* mice, which harbor a loss of function mutation in the $\beta_4$ subunit of VDCCs, exhibited a significant shift in LP luminance response, establishing a role for $Ca^{2+}$ in LP generation. When stimulated with ATP, which increases $[Ca^{++}]_I$, retinal pigment epithelial cells derived from $Vmd2^{-/-}$ mice exhibited a fivefold greater response than $Vmd2^{+/+}$ littermates, indicating that best-1 can suppress the rise in $[Ca^{2+}]_I$ associated with the LP. We conclude that VDCCs regulated by a $\beta_4$ subunit are required to generate the LP and that best-1 antagonizes the LP luminance response potentially via its ability to modulate VDCC function. Furthermore, we suggest that the loss of vision associated with BMD is not caused by the same pathologic process as the diminished LP, but rather is caused by as yet unidentified effects of best-1 on other cellular processes.

The Journal of General Physiology

## INTRODUCTION

In response to a light stimulus, the first components of the electroretinogram (ERG) that can be recorded are generated by neuronal elements of the retina (Robson and Frishman, 1995; Kofuji et al., 2000; Robson et al., 2003). These initial components are then followed by a series of slow changes in potential that are generated by nonneuronal retinal cells (Steinberg et al., 1985). The positive polarity c-wave represents the sum of two components of opposite polarity that are generated in response to the decline in subretinal $[K^+]$ associated with the retinal response to light, and is followed by the fast oscillation (FO), which is generated in part by the recovery of the c-wave and a $Cl^-$-induced hyperpolarization of the basal membrane of the retinal pigment epithelium (RPE) (Griff and Steinberg, 1984; Linsenmeier and Steinberg, 1984; Steinberg et al., 1985). The light peak (LP) follows the FO and reflects a depolarization of the basal membrane of the RPE due to an increased $Cl^-$ conductance (Linsenmeier and Steinberg, 1983; Steinberg et al., 1985; Gallemore and Steinberg, 1989). In contrast to the c-wave and FO, the LP arises independent of the change in subretinal $[K^+]$ that accompanies phototransduction. Instead, the LP is signaled by an as yet unidentified light peak substance (LPS) that is presumed to be secreted by photoreceptors (Gallemore et al., 1998). One candidate for the LPS is ATP, which, when applied to RPE cells in vitro, causes a $Ca^{2+}$-dependent increase in the $Cl^-$ conductance across the RPE basal membrane that is highly reminiscent of the LP (Peterson et al., 1997).

Clinically, the LP is measured by electrooculography (EOG), a test that is used to monitor drug toxicity effects on the RPE and is also considered the defining diagnostic test for Best vitelliform macular dystrophy (BMD). BMD is caused by mutations in the *VMD2* gene.

Correspondence to Alan D. Marmorstein: amarmorstein@eyes.arizona.edu

Abbreviations used in this paper: ADVIRC, autosomal dominant vitreoretinal choroidopathy; AVMD, adult onset vitelliform dystrophy; BMD, Best vitelliform macular dystrophy; DC, direct current; EOG, electrooculogram; ERG, electroretinogram; FO, fast oscillation; LP, light peak; LPS, LP substance; VDCC, voltage-dependent calcium channel; wt, wild-type.

It is an autosomal dominant inherited disease characterized by early onset degeneration of the macula (Godel et al., 1986), a specialized central region of the retina necessary for high acuity vision. The pathogenesis of BMD is characterized clinically by an egg yolk–like vitelliform lesion in the ocular fundus (Marmor, 1979; Gass, 1997) which typically presents in childhood. Eventually the vitelliform lesion will become disrupted and atrophic. Postmortem studies of donor eyes typically indicate substantial abnormal accumulation of lipofuscin in the RPE (Frangieh et al., 1982; Weingeist et al., 1982; O'Gorman et al., 1988), though exceptions have been reported (Mullins et al., 2005). Not all carriers of BMD-associated mutations develop vitelliform lesions and vision loss. The only fully penetrant symptom of the disease is the finding of a diminished LP without aberrations in the a- or b-waves of the flash ERG (Deutman, 1969; Cross and Bard, 1974). Historically the EOG has been the diagnostic determinant that distinguishes BMD from adult onset vitellifrom dystrophy (AVMD) (Marmor, 1979), though mutations in VMD2 have been reported in AVMD patients (Allikmets et al., 1999; White et al., 2000; Seddon et al., 2001).

Mutations in *VMD2* have also been found in autosomal dominant vitreoretinochoroidopathy (ADVIRC) (Yardley et al., 2004). ADVIRC is characterized by specific defects in pigmentation accompanied by choroidal atrophy and the presence of yellow-white retinal opacities (Blair et al., 1984). Abnormalities in the LP have also been observed (Han and Lewandowski, 1992) in ADVIRC patients. These abnormalities however are accompanied by a subnormal flash ERG response (Han and Lewandowski, 1992).

The *VMD2* gene encodes bestrophin (best-1), a 68-kD member of the bestrophin or RFP-TM family of proteins. Although mRNA for best-1 is in RPE, testis, placenta, and brain, (Petrukhin et al., 1998; Marquardt et al., 1998), the protein has only been detected in RPE cells (Stanton et al., 2006), where it is localized to the basolateral plasma membrane (Marmorstein et al., 2000; Bakall et al., 2003). Understanding best-1 function should be a key toward identifying candidate therapies for BMD. The EOG LP abnormality has served for many in the field as the basis to hypothesize a function for best-1. Studies performed in the Steinberg laboratory have shown that the LP is generated by a depolarization of the basal plasma membrane due to activation of a $Cl^-$ conductance (Gallemore and Steinberg, 1989). Based on the symptoms of BMD and the localization of the protein, the simplest hypothesis for best-1 function is that the LP is generated by a single $Cl^-$ channel, that best-1 is that channel, and that the disease is due to loss of best-1 $Cl^-$ channel activity. Evidence in favor of this hypothesis was first provided by Sun et al. (2002). In that study, heterologous expression of various bestrophins in HEK 293 cells resulted in the appearance of $Ca^{2+}$-sensitive $Cl^-$ currents that were not observed or were significantly smaller when BMD-associated mutants were introduced. Subsequent patch-clamp studies in transfected cells (Qu et al., 2003; Tsunenari et al., 2003) have found that different bestrophin family members have unique I/V relationships (Qu et al., 2003; Tsunenari et al., 2003; Qu et al., 2004), and have identified amino acid residues that appear to confer ion selectivity in transfected cells (Qu et al., 2004; Qu and Hartzell, 2004). A consistent finding has been that the introduction of mutations that cause BMD at conserved positions in the amino acid sequence results in a loss of diminished level of channel activity. These data have resulted in a model of BMD pathogenesis that explains the diminished LP and histopathologic consequences as the result of reduced or absent best-1 $Cl^-$ channel activity (Sun et al., 2002). We have recently shown that rats overexpressing BMD-associated best-1 mutants exhibit a diminished LP and an altered luminance response function (Marmorstein et al., 2004). However, overexpression of wild-type (wt) best-1 did not increase LP amplitude, as might be predicted based on other studies of $Cl^-$ channel overexpression (Zhou et al., 1994; Wersto et al., 1996), but did appear to reduce the sensitivity of the LP generator to light (Marmorstein et al., 2004).

In the present study, we sought to test the hypothesis that best-1 is the generator of the LP response by disrupting the *Vmd2* gene in mice. Surprisingly, in comparison to wt littermates, *Vmd2*$^{-/-}$ mice have a normal maximum LP but exhibit larger LPs in response to lower intensity stimuli. We also noted that the LP can be diminished by nimodipine, a blocker of L-type voltage-dependent calcium channels (VDCCs), and that *lethargic* mice harboring a loss of function mutation in the VDCC $\beta_4$ subunit (Burgess et al., 1997) exhibit significant shifts in LP responses across a broad range of stimulus luminance, but have otherwise normal retinal function. Finally we demonstrate that *Vmd2*$^{-/-}$ mice exhibit normal $Ca^{2+}$-activated $Cl^-$ conductances, but that the change in $[Ca^{2+}]_I$ in *Vmd2*$^{-/-}$ mice elicited by extracellular ATP is substantially elevated in comparison to wt littermates. Based on these findings, we conclude that VDCCs containing a $\beta_4$ subunit are required to generate a normal LP, and that best-1 is not required to generate the LP, but in fact functions to antagonize the LP luminance response by regulating $[Ca^{2+}]_I$ perhaps via its effects on the kinetics of VDCCs (Rosenthal et al., 2006).

## MATERIALS AND METHODS

### Targeted Disruption of the Vmd2 Gene

A BAC clone containing the entire mouse genomic DNA for *Vmd2* was isolated by screening a genomic 129/SvJ mouse library (Incyte Genomics). A replacement targeting vector was constructed using

a 4.8-kb EcoRI-AvrII fragment corresponding to a region upstream of *Vmd2* coding region and a 3-kb XbaI-BamHI fragment spanning introns I–III as the 5′ and 3′ arms of homology, respectively. Both fragments were subcloned into the vector PGKneolox-2DTA (a gift from P. Soriano, Fred Hutchinson Cancer Research Center, Seattle, WA). The neomycin phosphotransferase gene ($Neo^r$) under control of the mouse phosphoglycerate kinase I (PGK) promoter was inserted in inverse orientation with respect to the endogenous *Vmd2* gene. This targeting vector also contains an expression cassette of bacterial dipheria toxin A fragment (DTA) for negative selection. The targeting construct was linearized using a unique MluI restriction site and electroporated into 129/SvJ ES cells (Cell and Molecular Technologies). Homologous recombination was determined by Southern blot analysis. Homologous recombination between the wt locus and the targeting vector resulted in the replacement of 3 kb of genomic DNA, including 500 bp upstream of the start codon and the first protein-coding exon. ES cell clones were injected into C57BL/6 blastocysts to produce chimeras. Chimeras were bred with 129SvJ and C57BL/6 females, respectively. Heterozygotes identified by Southern blot analysis of tail DNA were inbred to yield $Vmd2^{-/-}$ homozygous mutants.

### RT-PCR

RT-PCR was performed to confirm the absence of *Vmd2* gene expression in $Vmd2^{-/-}$ mice. Total RNA was isolated from the posterior poles of mouse eyes using Trizol (Invitrogen) and reverse transcribed using oligo dT15 as primer. In PCR reactions, primers corresponding to the mouse best-1 cDNA sequence were used (5′-CAAGCTTCCACCATGACTATCACCTACACAAACA-3′ and 5′-CACGGCAAGTTCTCGTACTG-3′). These primers span different exons to distinguish PCR products for cDNA from genomic DNA contamination by the size difference in fragment length. Primers corresponding to fibulin-3 were used as a positive control for RNA integrity.

### VDCC Mutant Mice

Mice lacking either the $\beta_1$ or $\beta_2$ subunit of VDCCs were generated using gene targeting and transgenic rescue, as described elsewhere (Gregg et al., 1996; Ball et al., 2002). Mice heterozygous for the *lethargic* defect were obtained from The Jackson Laboratory and bred to obtain the mice tested here.

### Electroretinography

After overnight dark adaptation, mice were anesthetized with ketamine (80 mg/kg) and xylazine (16 mg/kg). Eye drops were used to anesthetize the cornea (1% proparacaine HCl) and to dilate the pupil (1% mydriacyl, 2.5% phenylephrine HCl, 1% cyclopentolate HCl). Mice were placed on a temperature-regulated heating pad throughout the recording session. All procedures involving animals were approved by the local institutional animal care and use committees and were in accordance with the Institute for Laboratory Animal Research Guide for Care and Use of Laboratory Animals.

Two stimulation and recording systems and protocols were used. ERG components generated by the RPE were recorded as described previously (Peachey et al., 2002; Wu et al., 2004a,b). Each mouse was tested only once on a given day, using only a single stimulus condition, and intensity–response functions were developed from multiple recording sessions that were separated by at least 2 d. The unattenuated stimulus was 4.4 log cd/$m^2$, corresponding to 6.8 log photoisomerizations/rod/s (Wu et al., 2004b).

The major components of the dc-ERG were measured conventionally (Peachey et al., 2002; Wu et al., 2004a,b). The amplitude of the c-wave was measured from the prestimulus baseline to the peak of the c-wave. The amplitude of the FO was measured from the c-wave peak to the trough of the FO. The amplitude of the LP was measured from the FO trough to the asymptotic value. The amplitude of the off-response was measured from the tail of the response to the peak of the off-response, which is either negative or positive in polarity, depending on flash intensity (Wu et al., 2004a,b).

Conventional ERG responses were recorded using a stainless steel electrode that made contact with the corneal surface through a thin layer of 0.7% methylcellulose. Needle electrodes placed in the cheek and the tail served as reference and ground leads, respectively. Under these conditions, mice typically develop reversible cataracts. Responses were differentially amplified (0.3–1,500 Hz), averaged, and stored using a UTAS E-3000 signal averaging system (LKC Technologies). ERGs were recorded to flash stimuli presented in an LKC ganzfeld. The maximulus stimulus intensity used was 2.1 log cd s/$m^2$, equivalent to 4.5 log photoisomerizations/rod/s (Wu et al., 2004b). At each flash intensity, interstimulus intervals were chosen to maintain a stable level of response, and increased from 4 s at the lowest flash intensity to 61 s at the highest stimulus levels.

The amplitude of the a-wave was measured from the prestimulus baseline to the a-wave trough. The amplitude of the b-wave was measured from the a-wave trough to the peak of the b-wave or, if no a-wave was present, from the prestimulus baseline. Implicit times were measured from the time of flash onset to the a-wave trough or the b-wave peak.

### Immunohistochemistry

Adult mouse eyes were fixed overnight in 4% paraformaldehyde in PBS and processed for paraffin embedding as described previously (Bakall et al., 2003). Following antigen retrieval, sections were stained with polyclonal anti-mouse best-1 antibody PAB-003 as described previously (Bakall et al., 2003) using DAB as substrate. Sections were counterstained with nuclear fast red and examined and photographed using a Nikon E600 microscope with CCD camera.

### Isolation of Fresh RPE Cells

Eyes of 2–3-mo-old mice were enucleated and opened by a circumferential incision along the *ora serrata*. After removal of the anterior parts of the eye including retina, the RPE layer was washed and incubated in $Mg^{2+}$ and $Ca^{2+}$ PBS for 5 min. Sheets of RPE were removed using a pair of fine forceps. These RPE sheets were directly subjected for measurements of intracellular free $Ca^{2+}$. To prepare a single cell suspension for patch-clamp analysis, RPE cell sheets were incubated in papain (0.5 U/ml) for 20 min and dissolved into a single cell suspension by gentle pipetting. The papain reaction was stopped using DMEM cell culture medium with 0.1% FCS.

### Patch-clamp Recordings of Whole Cell $Cl^-$ Currents

Fresh RPE cells from the single cell suspensions were placed in a bath chamber on the stage of an inverted microscope and were allowed to settle for 30 min. $Cl^-$ currents were measured in $K^+$-free solutions. The bath solution was composed of (in mM) 136.43 NaCl, 1,1 $Na_2HPO_4$, 4.17 $NaHCO_3$, 0.89 $MgCl_2$, 0.95 $CaCl_2$, 5.8 TEACl, 25 HEPES, 11.1 glucose, adjusted to pH 7.4 with Tris. Patch-clamp electrodes with a resistance of 3–5 MΩ were pulled from borosilicate glass using a DMZ Universal Puller. The electrodes were filled with a solution containing (in mM) 100 CsCl, 10 NaCl, 2 $MgSO_4$, 0.5 $CaCl_2$, 5,5 EGTA, HEPES, adjusted to pH 7.2 with Tris. This solution has a calculated concentration of free $Ca^{2+}$ of 10 nM. To ensure that recorded currents were bona fide $Cl^-$ currents, in some experiments $E_{Cl}$ was varied by replacing extracellular $Cl^-$ with $I^-$. This was accomplished by substituting NaI for NaCl and resulted in a shift of the reversal potential from 1.3 ± 2.2 mV toward more negative values (by −8.4 ± 1.5 mV, $n = 4$ cells). The authenticity of $Cl^-$ currents was further validated

by their sensitivity to 1 mM DIDS, which reduced current amplitude by 53 ± 6% (mean ± SD, $n = 4$).

To compare ion currents in the presence of elevated $Ca^{2+}$, the same pipette solution with 400 nM without EGTA was used. Whole-cell currents were measured using an EPC-9 (HEKA) patch-clamp amplifier in conjunction with TIDA hard and software (HEKA) for data acquisition and analysis. Membrane and access resistance were compensated for by the patch-clamp amplifier. The mean membrane capacitance in RPE cells from *Vmd2*$^{+/+}$ mice was 57.6 ± 39 pF (mean ± SD; $n = 41$) and in *Vmd2* $^{-/-}$ mice 51.3 ± 35.3 pF (mean ± SD; $n = 10$). The access resistance was compensated for to values smaller than 10 MΩ.

### Measurements of Intracellular Free $Ca^{2+}$

Intracellular free $Ca^{2+}$ was measured using the $Ca^{2+}$-sensitive fluorescent dye fura-2 according to the method of Grynkiewicz et al. (1985). Fluorescence of fura-2 was measured using a Visitron Systems polychromator and fluorescence detection system connected to a Carl Zeiss MicroImaging, Inc. inverted microscope. During the measurements, the cells were superfused by bath solution composed of (in mM) 118 NaCl, 5 KCl, 1.2 $MgCl_2$, 1.2 $Na_2SO_4$, 2 $NaH_2PO_4$, 1.8 $CaCl_2$, 9.1 glucose, 21 HEPES, pH 7.4 adjusted with Tris. For fura-2 loading, sheets of freshly isolated RPE cells were incubated for 45 min in bath containing 10 μM fura-2-AM. Absolute values of intracellular free $Ca^{2+}$ were estimated using intracellular calibration according to Grynkiewicz et al. (1985) using bath solution with 10 μM ionomycin to saturate fura-2 with $Ca^{2+}$ and $Ca^{2+}$-free bath solution with 10 μM ionomycin to deplete fura-2 from $Ca^{2+}$. $Ca^{2+}$ concentrations were calculated using Visitron software.

## RESULTS

### Generation of Mice with a Disrupted Vmd2 Gene

We disrupted the *Vmd2* locus by homologous recombination in mouse ES cells using a replacement vector (Fig. 1 A). The deleted genomic sequence encompasses a region beginning 500 bp upstream of the initiation codon and including all of exon 1. The generation of a null mutant was confirmed by Southern blot (Fig. 1, B and C), RT-PCR, and by immunohistochemistry

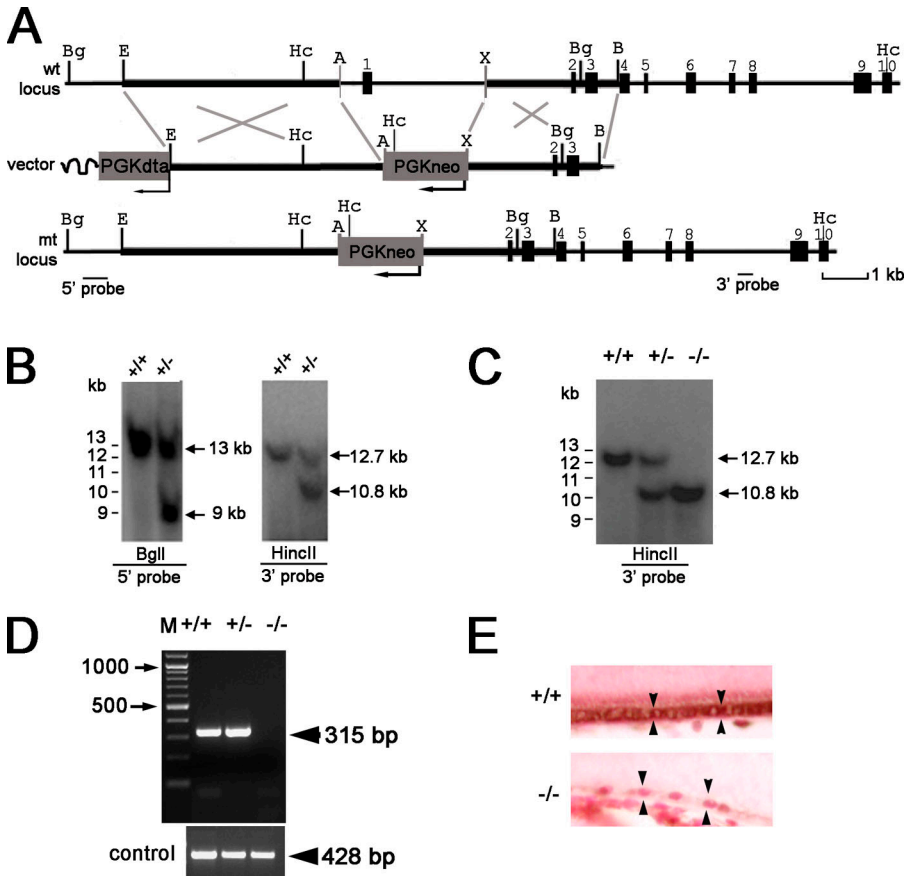


**Figure 1.** Targeted disruption of the *Vmd2* gene. A schematic diagram of the wild-type (wt) locus, targeting vector, and mutant (mt) locus is presented in A. Thick lines represent fragments used for constructing the targeting vector 5′ and 3′ arms. Numbered solid boxes depict *Vmd2* exons. The neo$^r$ and DTA gene expression cassettes are indicated by the labeled gray boxes. The drawing line represents plasmid vector sequence. The external 3′ probe used in B is indicated beneath the mt locus. Restriction enzyme sites: Bg, BglI; E, EcoRI; Hc, HincII; A, AvrII; X, XbaI; B, BamHI. Southern blot analysis of wt (*Vmd2*$^{+/+}$), heterozygous (*Vmd2*$^{+/-}$), and homozygous (*Vmd2*$^{-/-}$) mouse tail genomic DNA digested with HincII (B and C). The wt fragment is 12.7 kb and the mt fragment is 10.8 kb. RT-PCR analysis of total RNA was used to confirm a null phenotype (D). The 315-bp *Vmd2*-derived PCR product was present in *Vmd2*$^{+/+}$ and *Vmd2*$^{+/-}$ mice but absent in the $^{-/-}$ lane. In the positive control, a 428-bp product was obtained from all mice using primers for fibulin-3. Best-1 was detected by immunohistochemistry in the RPE of *Vmd2*$^{+/+}$ but not *Vmd2*$^{-/-}$ mice (E). Arrows in E indicate the RPE.

using an anti-mouse best-1 antibody as described previously (Bakall et al., 2003). When examined by RT-PCR, no band was detected using total RNA from *Vmd2*$^{-/-}$ mice, while *Vmd2*$^{+/+}$ and *Vmd2*$^{+/-}$ mice were positive for the predicted 315-bp PCR product (Fig. 1 D). Immunohistochemical staining of eyes with an antibody directed at the COOH terminus of mouse best-1 reproduced the localization of best-1 (Bakall et al., 2003) to RPE cells in *Vmd2*$^{+/+}$and $^{+/-}$ mice, while *Vmd2*$^{-/-}$ mice exhibited no staining (Fig. 1 E).

*Vmd2*$^{-/-}$ mice were viable, grew normally, were fertile, and demonstrated no obvious physical or behavioral abnormalities. No histological evidence of retinal degeneration was noted in *Vmd2*$^{-/-}$ mice as old as 14 mo of age.

### Analysis of the ERG Phenotype in Vmd2$^{-/-}$ Mice

The only fully penetrant symptom of BMD is a diminished LP with an otherwise normal a- and b-wave of the flash ERG, which is performed on dark-adapted subjects and measures rod driven responses (Robson and Frishman, 1998). We examined dark-adapted ERG responses in *Vmd2*$^{-/-}$ mice. No significant differences were observed in the amplitude (Fig. 2 A) or implicit time (Fig. 2 B) of the rod a- or b-waves of *Vmd2*$^{-/-}$ mice compared with *Vmd2*$^{+/+}$ mice under any stimulus condition.

The EOG LP can be monitored more precisely using direct current (DC) amplification of the ERG (Steinberg et al., 1985). To assess the role of best-1 in the LP we recorded DC-ERGs across a 5-log unit range of stimulus luminance from adult mice aged 2–6 mo. At the three lowest stimulus luminance levels (−1, 0, and 1 log cd/m$^2$), significantly ($P < 0.05$) larger LPs were recorded from *Vmd2*$^{-/-}$ mice relative to *Vmd2*$^{+/+}$ mice (Fig. 3). Notably, at the lowest stimulus applied, *Vmd2*$^{+/+}$ mice exhibited responses that were barely discernable from baseline, while *Vmd2*$^{-/-}$ mice exhibited LPs with amplitudes between 300 and 400 μV. At higher stimulus luminance levels, amplitudes were similar in *Vmd2*$^{+/+}$ and *Vmd2*$^{-/-}$ mice. *Vmd2*$^{+/-}$ mice exhibited responses that did not differ significantly from those of *Vmd2*$^{+/+}$ mice (unpublished data). These findings indicate that best-1 is not required to generate the ionic conductances that underlie the LP, and suggest that it antagonizes the LP response. Limited recordings from animals up to 14 mo of age showed similar effects with no deficits in the responses (unpublished data).

The c-wave and FO of *Vmd2*$^{+/+}$ and *Vmd2*$^{-/-}$ mice were indistinguishable at all stimulus luminance levels tested. Interestingly, a difference in the off-response was noted. Although the origin of this response component is unknown, the polarity of the off-response reverses, from negative to positive, with increasing stimulus intensity (Wu et al., 2004a,b). While the off-response amplitudes in both *Vmd2*$^{+/+}$ and *Vmd2*$^{-/-}$ mice were similar, the reversal of response polarity occurred at a lower stimulus luminance in *Vmd2*$^{-/-}$ mice than in *Vmd2*$^{+/+}$ or *Vmd2*$^{+/-}$ littermates. This shift is consistent with the enhanced LP observed in response to lower intensity stimuli.

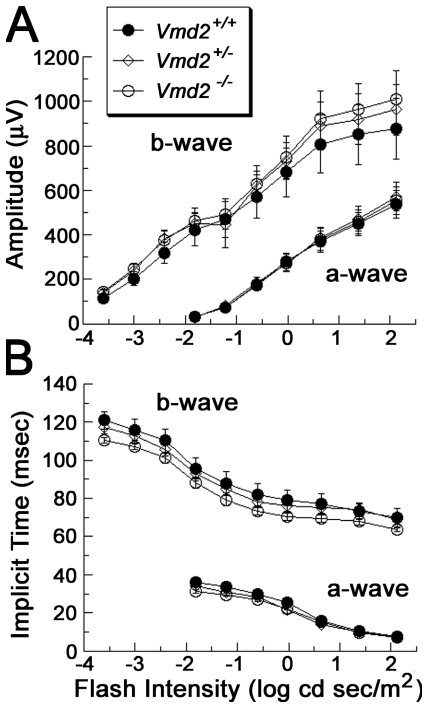


**Figure 2.** Effect of *Vmd2* disruption on the flash ERG. Amplitude (A) and implicit time (B) of the a-wave and b-wave components of the dark-adapted strobe flash ERG plotted as a function of stimulus intensity. Symbols indicate the mean ± SEM result of six mice.

### Analysis of Whole Cell Cl$^-$ Conductances

Since best-1 has been described to function as a Cl$^-$ channel, we analyzed RPE cells freshly isolated from *Vmd2*$^{+/+}$ and *Vmd2*$^{-/-}$ mice for possible differences in whole cell Cl$^-$ conductance using whole cell patch-clamp. Isolated cells possessed properties similar to those described for freshly isolated rat RPE by Ueda and Steinberg (1994) with clearly discernable apical and basolateral membrane domains (Fig. 4 A). Our recordings were initially performed in buffer containing a low [Ca$^{2+}$], resulting in an intracellular free [Ca$^{2+}$] of 10 nM. When subjected to a series of voltage steps as indicted in Fig. 4 B, most of the cells showed inwardly rectifying currents for both *Vmd2*$^{+/+}$ and *Vmd2*$^{-/-}$ mice (Fig. 4, C and D). In some cells, an outwardly rectifying conductance was also recorded, though this was seen in cells derived from *Vmd2*$^{+/+}$ or *Vmd2*$^{-/-}$ mice. Under low [Ca$^{2+}$] conditions, no difference in current density was observed between *Vmd2*$^{+/+}$ and *Vmd2*$^{-/-}$ mice. Since best-1 has been described as a Ca$^{2+}$-dependent Cl$^-$ channel, we also performed whole-cell recordings with an intracellular Ca$^{2+}$ concentration of 400 nM. This condition has been used by others to stimulate

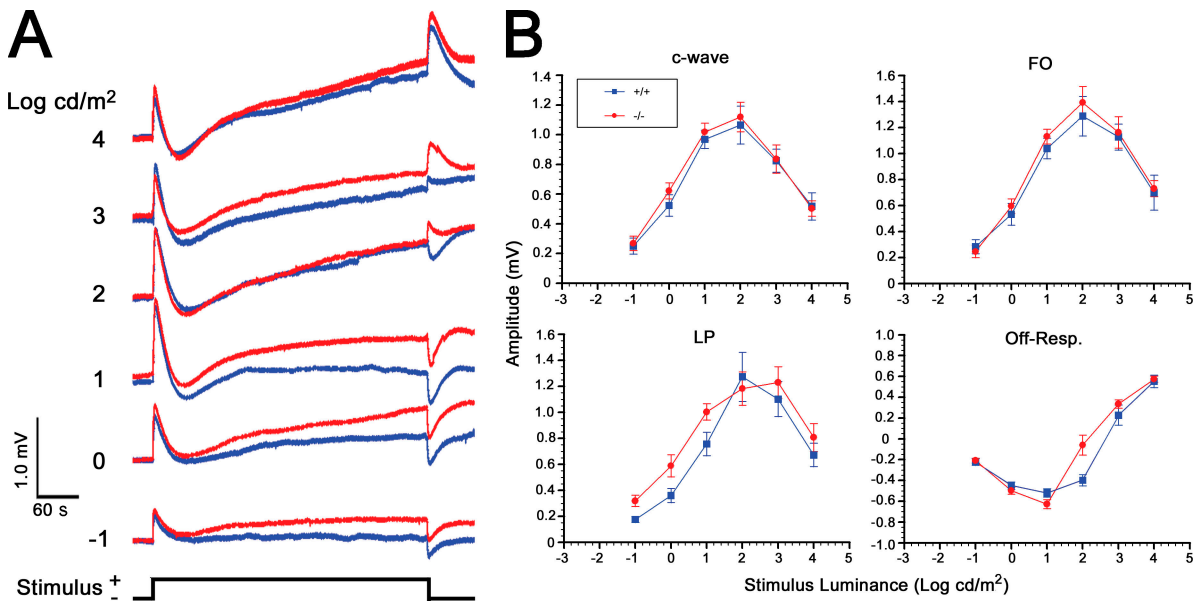


**Figure 3.** Effect of *Vmd2* disruption on RPE-generated ERG components. ERGs were recorded to 7-min duration stimulus flashes from $Vmd2^{+/+}$ (blue) and $Vmd2^{-/-}$ (red) mice. Grand average of responses obtained from ≥15 individual mice are shown in A for each stimulus intensity. Stimulus presentation is represented by the lower trace (black). Intensity–response functions (B) for the amplitude of the major ERG components generated by the RPE in response to light. Data points indicate the mean ± SEM of >15 responses obtained from different mice.

best-1–associated currents (Fischmeister and Hartzell, 2005). High [$Ca^{2+}$] resulted in increased $Cl^-$ currents in RPE cells isolated from both $Vmd2^{+/+}$ and $Vmd2^{-/-}$ mice (Fig. 4, C–E); however, we did not observe any difference in the current density between $Vmd2^{+/+}$ and $Vmd2^{-/-}$ mice (Fig. 4 E). We conclude from these experiments that best-1 is not a dominant $Cl^-$ channel species in the RPE plasma membrane.

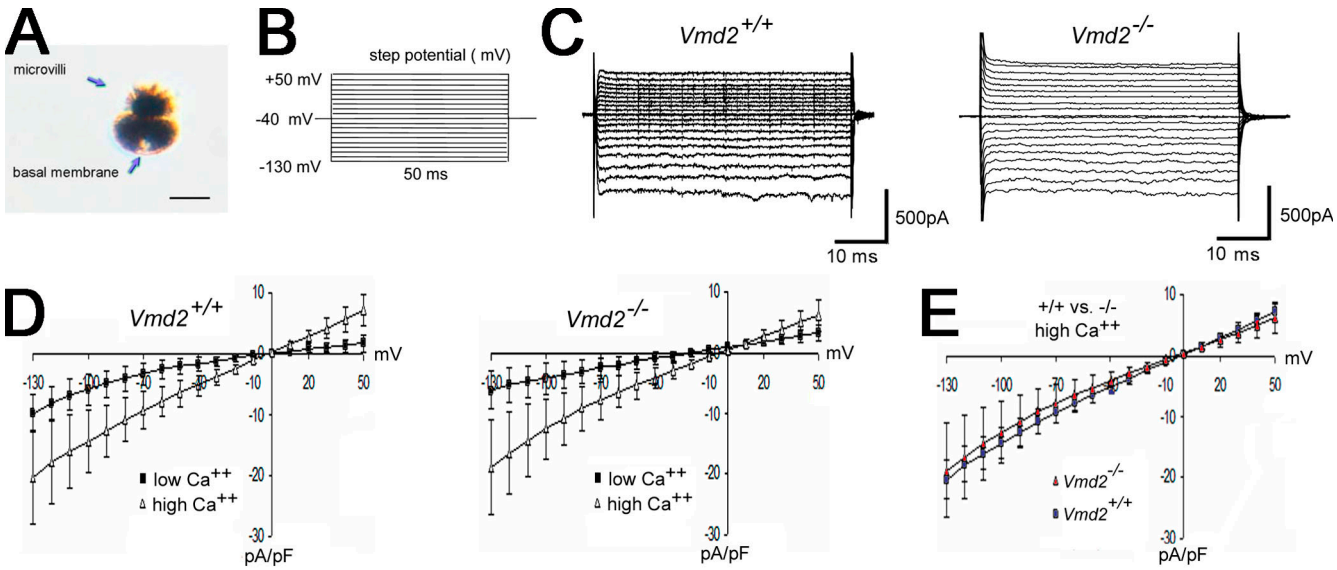


**Figure 4.** $Cl^-$ conductances in RPE cells isolated from $Vmd2^{+/+}$ and $Vmd2^{-/-}$ mice. RPE cells were isolated from mice as described in the Materials and Methods. As reported by Ueda and Steinberg (1994), apical microvilli could be distinguished from the basal surface of the cells as shown in A. $Cl^-$ currents in response to a series of step potentials (B) were analyzed by whole cell patch-clamp in low (10 nM) or high (400 nM) $Ca^{2+}$. Examples of recordings obtained from individual cells in high $Ca^{2+}$ are shown in C for both $Vmd2^{+/+}$ and $Vmd2^{-/-}$ mice. I/V plots for low and high $Ca^{2+}$ conditions are shown in D for both $Vmd2^{+/+}$ and $Vmd2^{-/-}$ mice (mean ± SD, $6 \leq n \leq 22$ cells). Note that larger currents were obtained in high $Ca^{2+}$ conditions. A comparison of currents obtained in high $Ca^{2+}$ conditions (E) indicates no differences between $Vmd2^{+/+}$ and $Vmd2^{-/-}$ mice.

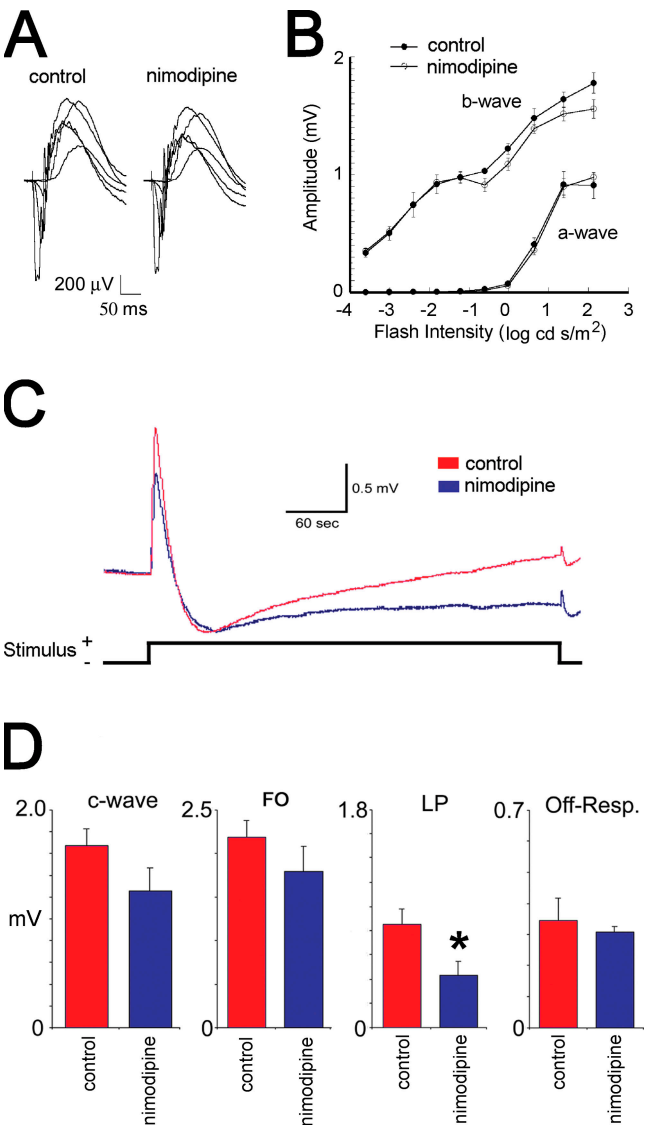


**Figure 5.** Effect of $Ca^{2+}$ channel blocker nimodipine on RPE-generated ERG components. The effect of nimodipine on the DC-ERG of *Vmd2*$^{+/+}$mice was determined 30 min after intraperitoneal injection of a 1 mg/kg dose of nimodipine using a 2 log cd/m$^2$ stimulus. Representative ERGs (A) obtained after injection of vehicle alone (control) or 1 mg/kg nimodipine. Intensity–response functions for major ERG components are shown in B. Each data point indicates the average (±SD) for three mice. The amplitude of the a-wave was measured 8 ms after stimulus presentation. The amplitude of the b-wave was measured to the peak of the b-wave from the a-wave trough or, if no a-wave was present, from the baseline. C shows grand average dc-ERG waveforms generated from animals receiving nimodipine or vehicle alone ($n$ = 8 both groups). Note the obvious reduction in amplitude of the LP in nimodipine-treated mice. C-wave, FO, LP, and off-response amplitudes are shown in D. Bars represent mean ± SEM.

### Effect of Nimodipine on the Light Peak

Since the LP of *Vmd2*$^{-/-}$ mice was not diminished or absent, and any effects on $Cl^-$ channel function were too weak for us to detect, we sought to better understand the basis of the LP response by studying the putative $Ca^{2+}$ sensitivity of the LP (Gallemore et al., 1998). The role of $Ca^{2+}$ in stimulating the LP was hypothesized based on the response of RPE cells to extracellular ATP (Peterson et al., 1997). We have recently shown that nimodipine, a specific inhibitor of L-type voltage-gated $Ca^{2+}$ channels, diminishes the LP of rats and that best-1 alters the kinetics of VDCCs (Rosenthal et al., 2006). On this basis, we analyzed the effects of nimodipine on the LP of *Vmd2*$^{+/+}$ and *Vmd2*$^{-/-}$ mice. Mice were injected intraperitoneally with nimodipine (1 mg/kg) or vehicle alone, and dark adapted for 30 min, after which DC-ERGs were recorded in response to a 2 log cd/m$^2$ stimulus. As shown in Fig. 5 and Fig. 6 (A and B), the LP was significantly reduced in *Vmd2*$^{+/+}$ and *Vmd2*$^{-/-}$ mice when compared with controls in which the animals were injected with vehicle alone. The reduction in LP amplitude was not the result of depressed photoreceptor function, as the a- and b-waves of the ERG were unaffected by nimodipine (Fig. 5, A and B). Furthermore, no difference in heart rate was observed between experimental and control groups (Table I). On average, treatment with nimodipine induced a significant decrease in LP amplitudes obtained to a 2 log cd/m$^2$ stimulus by 49.7% for *Vmd2*$^{+/+}$ mice ($P < 0.03$; $n = 8$) (Fig. 5, C and D) and 59.1% for *Vmd2*$^{-/-}$ animals ($P < 0.04$; $n = 8$) (Fig. 6, A and B). Since *Vmd2*$^{-/-}$ mice exhibit an enhanced luminance response, we also probed the effect of nimodipine at a stimulus luminance of −1 log cd/m$^2$ (Fig. 6, C and D). At this stimulus luminance, nimodipine caused a decrease of 47% ($p = 0.09$, $n = 5$) in LP amplitude with no change in c-wave, FO, or off-response in *Vmd2*$^{-/-}$ mice. *Vmd2*$^{+/+}$ did not mount an LP response of sufficient amplitude to measure at this stimulus luminance (see Fig. 3). These data suggest a potential role for VDCCs in determining LP amplitude, and suggest a greater sensitivity of the LP to nimodipine in *Vmd2*$^{-/-}$ mice.

### ERG Phenotypes in VDCC β Subunit Null Mice

We next set out to survey the RPE-generated components of the ERG in VDCC mutant mice. While the α1 subunit forms the ion pore, the specific $\alpha_1$ subunit(s) expressed in the mouse RPE are not known and α subunit knockout mice exhibit severe systemic phenotypes. In comparison, the β subunit is often required for correct localization and function of the $\alpha_1$ subunit

TABLE I

*Heart Rates (Beats per Minute) Determined before and after dc-ERG Recordings*

| | *Vmd2*$^{+/+}$ | | *Vmd2*$^{-/-}$ | |
|---|---|---|---|---|
| | Control | Nimodipine | Control | Nimodipine |
| Before dc-ERG | 243 ± 29 | 246 ± 28 | 269 ± 48 | 247 ± 56 |
| After dc-ERG | 281 ± 62 | 281 ± 32 | 297 ± 56 | 281 ± 57 |

Data are average ± SD. For each group $n = 8$.

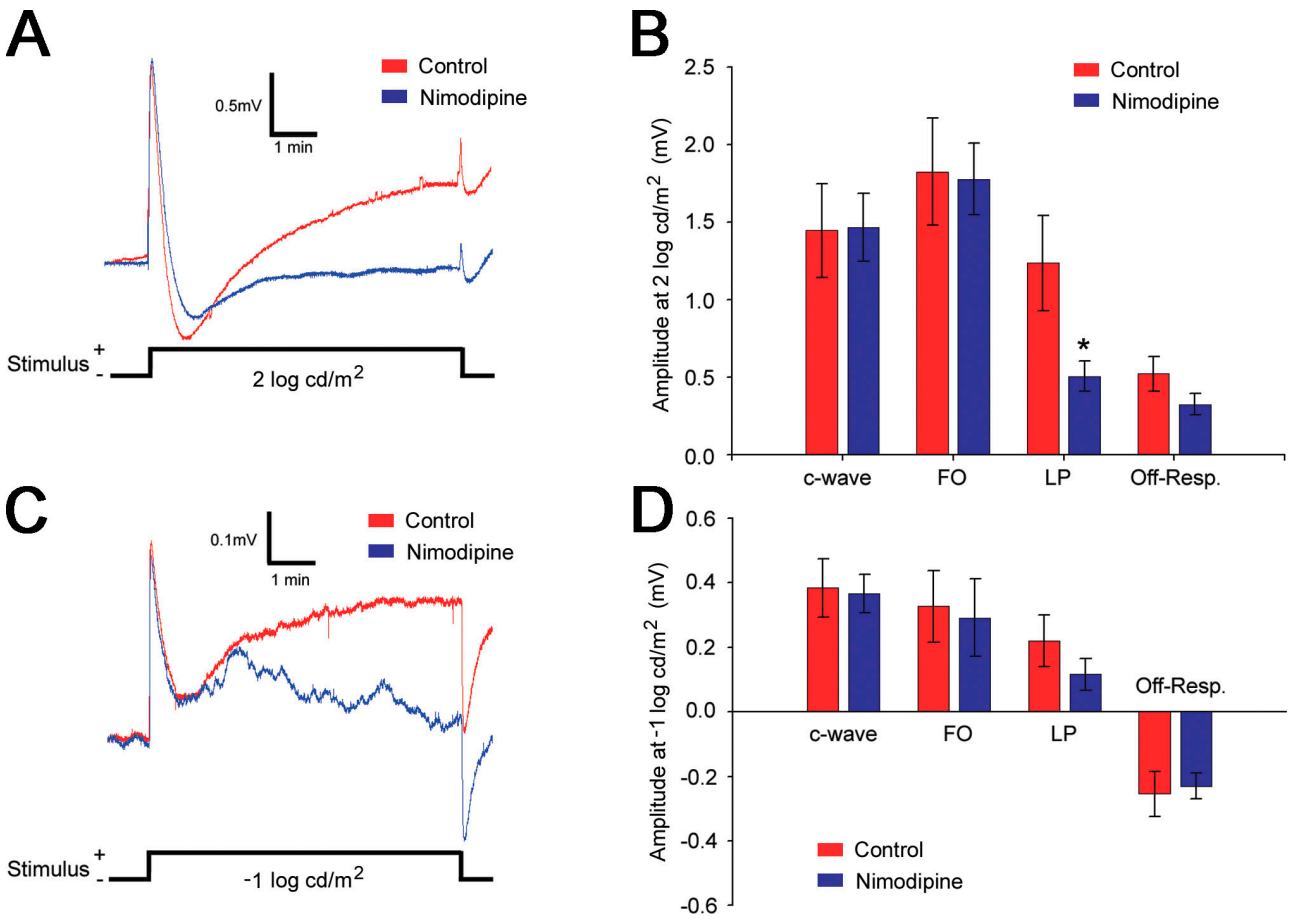


**Figure 6.** Effect of nimodipine on RPE-generated ERG components of *Vmd2*$^{-/-}$ mice. The effect of nimodipine on the DC-ERG of *Vmd2*$^{-/-}$mice was determined as indicated for *Vmd2*$^{+/+}$ mice in Fig. 5 using stimuli of 2 log cd/m$^2$ (A and B, $n = 8$) or $-2$ log cd/m$^2$ (C and D, $n = 5$). Examination of grand average waveforms (A and C) indicates that the most obvious effects are on the amplitude of the LP. Examination of maximum response amplitudes (B and D) confirms that there is minimum effect of nimodipine on the c-wave, FO, or off-response. However, the LP was significantly (*, $P < 0.05$) diminished at 2 log cd/m$^2$ (B). Although the LP was reduced at $-2$ log cd/m$^2$ (D), the effect was of borderline significance ($P = 0.09$). Data in C and D are mean ± SEM.

(Gregg et al., 1996; Burgess et al., 1999; Ball et al., 2002), and a survey of public SAGE databases indicated that mRNA for the $\beta_1$, $\beta_2$, and $\beta_4$ subunits of VDCCs are expressed in RPE cells. Our prior study indicated that in the absence of these β subunits, photoreceptors respond normally to light and none of these animals exhibit signs of retinal degeneration (Ball et al., 2002). Since rod photoreceptor activity is comparable in each β mutant mouse, RPE responses are induced by a comparable initiating stimulus from rod photoreceptor activity. LP amplitudes were recorded from each β mutant mouse and the matching controls. No significant changes were seen in $\beta_1$ or $\beta_2$ mutant mice (unpublished data). In comparison, ERG components generated by the RPE were significantly reduced in *lethargic* mice (Fig. 7), which express a loss of function mutation in the $\beta_4$ subunit (Burgess et al., 1997).

Analysis of the luminance–response functions obtained from *lethargic* mice indicates difference in LP amplitudes at 0 ($P = 0.049$), 1 ($P = 0.070$), and 2 ($P = 0.038$) log cd/m$^2$ stimuli (Fig. 7). Interestingly the maximum LP amplitude never reaches that of their wt littermates (*lethargic* = 1.34 ± 0.16 mV obtained at 3 log cd/m$^2$ vs. wt = 1.73 ± 0.20 mV obtained at 2 log cd/m$^2$, mean ± SEM, $n \geq 7$). Furthermore, the LP luminance–response function of *lethargic* mice is shifted by ~1 log unit toward higher intensities from that of wt mice (Fig. 7), indicating an overall decrease in sensitivity. Maximum amplitudes of the c-wave and FO were also depressed in *lethargic* mice, but these differences did not reach statistical significance except at the 2 log cd/m$^2$ stimulus level (c-wave $P < 0.001$, FO $P < 0.02$). These data indicate that VDCCs specifically containing a $\beta_4$ subunit play a role in generating the LP and possibly other RPE-generated components of the ERG.

### Effect of Best-1 on $[Ca^{2+}]_i$

Although *Vmd2*$^{-/-}$ mice exhibit no apparent alteration in $Ca^{2+}$-induced $Cl^-$ currents, we have demonstrated

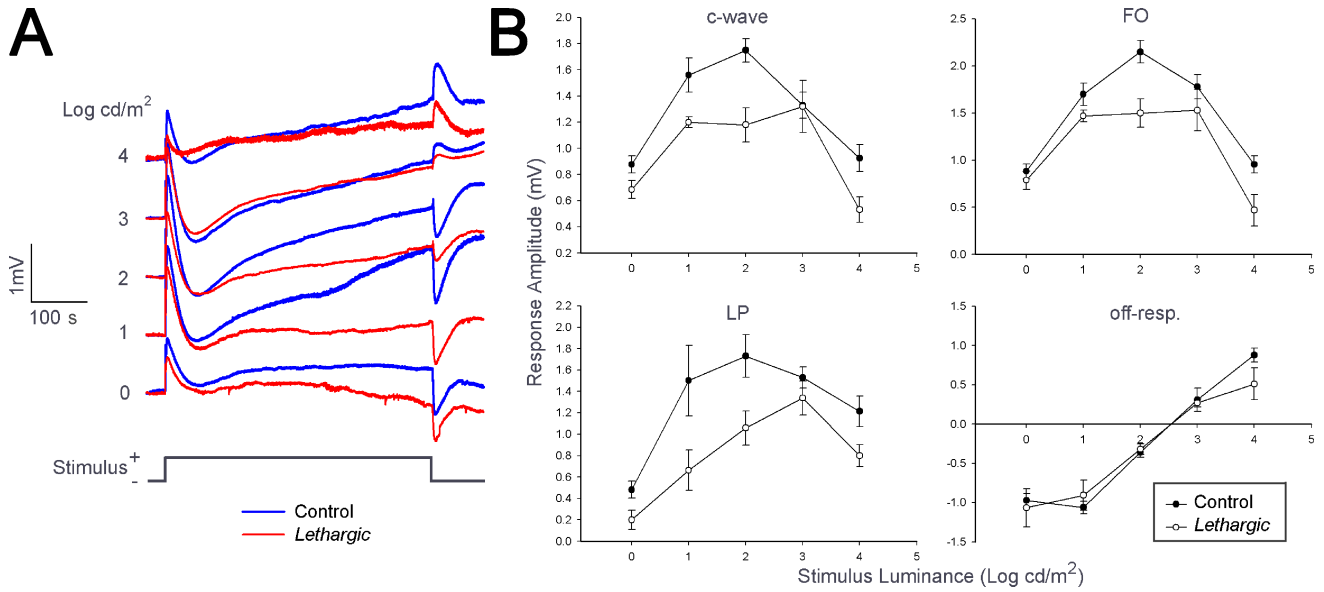


**Figure 7.** RPE-generated ERG components in the *lethargic* mouse. ERGs were recorded to 7-min duration stimulus flashes from control (blue) or *lethargic* (red) mice. Grand average of responses are shown in A for each stimulus intensity. Stimulus presentation is represented by the lower trace (black). Intensity–response functions (B) for the amplitude of the major ERG components generated by the RPE in response to light. Data points indicate the mean ± SEM. For luminance levels of 0 and 4 log cd/m$^2$, $n \geq 5$. For responses obtained at luminance levels of 1, 2, and 3 log cd/m$^2$, $n \geq 8$.

a role for $Ca^{2+}$ and VDCCs in generating the LP, and we have recently reported that best-1 can alter the kinetics of VDCCs (Rosenthal et al., 2006). Since extracellular ATP has been proposed to function as the LPS by changing both RPE $Cl^-$ conductance and $[Ca^{2+}]_I$ (Peterson et al., 1997; Mitchell, 2001; Reigada and Mitchell, 2005), we examined whether the absence of best-1 altered the RPE response to ATP. Changes in $[Ca^{2+}]_I$ were examined in freshly isolated sheets of RPE cells derived from either *Vmd2*$^{+/+}$ or *Vmd2*$^{-/-}$ mice loaded with the $Ca^{2+}$ indicator dye fura-2. Application of 100 μM ATP led to a slow monophasic rise in intracellular free $Ca^{2+}$ in RPE cells derived from either *Vmd2*$^{+/+}$ or *Vmd2*$^{-/-}$ mice (Fig. 8). The increase in $[Ca^{2+}]_I$ in *Vmd2*$^{-/-}$ RPE cells (to 280 ± 58% of resting levels) was significantly ($P < 0.05$) greater than that of *Vmd2*$^{+/+}$ RPE cells (to 126 ± 6% of resting level; Fig. 8 C).

## DISCUSSION

In this work, we set out to test the hypothesis that best-1 is the $Cl^-$ channel that generates the LP by disrupting the *Vmd2* gene. Based on this hypothesis, we predicted that the absence of best-1 expression should induce a marked reduction in this ERG component as well as a distinct reduction in the $Cl^-$ conductance of the cells recorded by whole cell patch-clamp in high $Ca^{2+}$. In contrast we found that LP responses in *Vmd2*$^{-/-}$ mice were actually larger at nonsaturating luminance levels than those recorded from *Vmd2*$^{+/+}$ mice (Fig. 3). In addition, we found no difference in $Cl^-$ conductances in *Vmd2*$^{-/-}$ vs. *Vmd2*$^{+/+}$ littermates, but we did observe a significant increase in the change in $[Ca^{2+}]_I$ elicited by stimulation with extracellular ATP in *Vmd2*$^{-/-}$ vs. *Vmd2*$^{+/+}$ littermates. These data indicate that best-1 is not required to generate the LP, and taken together with our previous findings that overexpression of best-1 in wt rats desensitizes the LP response (Marmorstein et al., 2004) and affects the kinetics of VDCCs (Rosenthal et al., 2006), can be interpreted as indicating that best-1 antagonizes the LP, thus predicting that disease-causing mutations of best-1 exhibit a gain of function in this regard.

### Generation of the LP

The LP arises from a depolarization of the basolateral plasma membrane of the RPE due to activation of a $Cl^-$ conductance. This response, in contrast to the c-wave and FO, is stimulated by an LPS that is thought to trigger the LP via a second messenger system involving $Ca^{2+}$ (Gallemore et al., 1998). The most likely candidate for the LPS is extracellular ATP, recognized at the apical plasma membrane by purinergic receptors (Peterson et al., 1997). Stimulation of RPE cells in vitro with ATP results in an increase in $[Ca^{2+}]_I$, resulting in the activation of a basolateral $Cl^-$ conductance similar to the LP (Peterson et al., 1997). Although the depletion of intracellular $Ca^{2+}$ stores occurs rapidly, the LP is sustained over several minutes. It is likely that some mechanism of extracellular $Ca^{2+}$ entry would be required to sustain the response, and it has been proposed that the LP $Cl^-$ conductance is activated

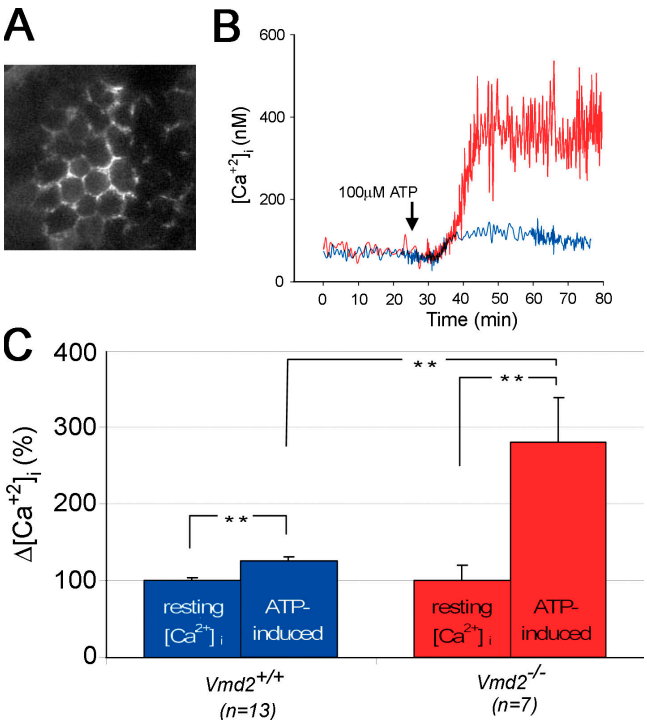


**Figure 8.** Effect of best-1 on changes in $[Ca^{2+}]_I$ in response to ATP stimulation. RPE sheets were isolated from the eyes of *Vmd2*$^{+/+}$ or *Vmd2*$^{-/-}$ mice (A) and loaded with fura-2. Changes in $[Ca^{2+}]_I$ were followed in response to stimulation with 100 μM ATP. Examples of data from individual cells are shown in B, where the red tracing is from cells isolated from *Vmd2*$^{-/-}$ mice and the blue tracing is from cells isolated from *Vmd2*$^{+/+}$ littermates. C indicates the maximum average percent change in $[Ca^{2+}]_I$ (average ± SD, $n = 13$ for *Vmd2*$^{+/+}$, $n = 7$ for *Vmd2*$^{-/-}$). **, $P < 0.05$.

(maintained) by an increase in $[Ca^{2+}]_I$ (Gallemore et al., 1998).

Consistent with a role of $Ca^{2+}$ in LP generation, LP amplitude is selectively reduced by the VDCC inhibitor nimodipine in rats (Rosenthal et al., 2006) and mice (Figs. 5 and 6). Since L-type channels can mediate capacitative $Ca^{2+}$ entry into cells (Putney et al., 2001; Mergler and Strauss, 2002), these findings led us to investigate the role of VDCCs in LP generation. *lethargic* mice were found to exhibit a substantial shift of the LP luminance response function and diminished maximum LP amplitudes in comparison to congenic controls. This places VDCCs regulated by the $\beta_4$ subunit in the LP response pathway and makes the $\beta_4$ subunit the first molecule experimentally demonstrated to be required to generate the LP.

The antagonistic effect of best-1 on the LP and its ability to suppress release of $[Ca^{2+}]_I$ would account for the desensitization effects observed when mutant best-1 is overexpressed in rats (Marmorstein et al., 2004) and suggests that best-1 may interact with VDCCs to regulate their responses. We have recently shown that best-1 can alter the kinetics of VDCCs (Rosenthal et al., 2006) and that BMD-associated best-1 mutants alter VDCC kinetics in different ways than the wt protein. However, whether best-1 interacts with VDCCs via physical interaction, signal transduction, or as a consequence of other activities in which best-1 participates awaits further investigation.

Having established a firm experimental link between $[Ca^{2+}]_I$, VDCCs, and the LP, we sought to determine whether best-1 affected the change in $[Ca^{2+}]_I$ elicited by a potential LPS, ATP. In comparison to *Vmd2*$^{+/+}$ littermates, the increase in $[Ca^{2+}]_I$ in RPE cells derived from *Vmd2*$^{-/-}$ mice stimulated with 100 μM ATP increased approximately fivefold.

### Is Best-1 an RPE Plasma Membrane $Cl^-$ Channel?

Despite considerable evidence that best-1 can function as a $Cl^-$ channel when expressed in vitro (for review see Hartzell et al., 2005), we found no indication that best-1 functions in this capacity in the RPE plasma membrane, generates the LP, or that best-1 is required for the health of the RPE or the retina. Since our analysis of $Cl^-$ currents in mouse RPE cells was not exhaustive (Fig. 4), we cannot on the basis of this data state conclusively that best-1 is not a $Cl^-$ channel, or exclude the possibility that another $Cl^-$ channel has compensated for the lack of best-1. However, we have recently demonstrated that mice lacking CFTR or carrying mutant (Δ508) CFTR exhibit impaired responses with regard to all RPE-generated ERG components, including the LP (Wu et al., 2006), but no change in the position of the LP luminance–response function. Furthermore, mice lacking CLC-2 exhibit a deficit in the transepithelial potential of the RPE (Bösl et al., 2001) and an early onset retinal degeneration. Thus, in the only other models in which $Cl^-$ channels have been removed from the RPE, there is no evidence for compensation by other channel types. Nevertheless, RT-PCR data suggest that best-2 may be expressed by the RPE, and it remains possible that best-2 may compensate for absence of best-1.

### Clinical Implications

From a clinical-genetic point of view, our data are not surprising. Mutations in *VMD2* cause BMD and ADVIRC, both of which exhibit a dominant pattern of inheritance. If disruption of best-1 $Cl^-$ channel activity were the cause of BMD, it would be likely that a disruption of the *VMD2* gene in the human population would also cause BMD or a more severe form of retinal degeneration and that a null mutant with a recessive pattern of inheritance would have been reported. No recessive disease associated with mutations in *VMD2* has, to date, been reported. In addition, AVMD is distinguished from BMD by the presence of a normal LP. Despite this, three mutations in the *VMD2* gene have been reported in patients diagnosed with AVMD on the

basis of EOG testing (http://www.uni-wuerzburg.de/humangenetics/vmd2.html) (Kramer et al., 2000). Of these mutations, T6P and A243T (A243V has not been studied) have impaired best-1–associated $Cl^-$ conductances (Sun et al., 2002).

Based on the defects in the LP of the *lethargic* mouse and the presence of putative loss of function mutations in AVMD patients, it seems unlikely that the diminished LP in BMD or ADVIRC results from a loss of best-1 $Cl^-$ channel activity. In this regard, it is interesting to note that although suffering from episodic ataxia and epilepsy, neither *lethargic* mice (Ball et al., 2002) nor humans with $\beta_4$ subunit mutations (Escayg et al., 2000) have been reported to exhibit retinal degeneration or other vision problems. Instead, our findings of enhanced LP responses in *Vmd2*$^{-/-}$ mice accompanied by an enhancement of ATP-induced $[Ca^{2+}]_I$, the diminished LP in *lethargic* mice without retinal defects, and the dominant inheritance patterns of BMD and ADVIRC suggest that the pathophysiology of vision loss in these diseases is due to a gain of function in best-1 and is independent of the effects on the LP.

In summary, based on the data that we have presented, we propose that best-1 is not necessary to generate the LP, but rather that it serves to antagonize it, possibly via its ability to inhibit increases in $[Ca^{2+}]_I$ in response to a stimulus, and by modulating VDCC kinetics (Rosenthal et al., 2006). We have also provided evidence indicating that VDCCs containing a $\beta_4$ subunit are a necessary component of the LP pathway. The absence of retinal degeneration in the *Vmd2*$^{-/-}$ mouse, in the *lethargic* mouse, and in humans with VDCC $\beta_4$ subunit mutations and the presence of vitelliform lesions in AVMD patients carrying *VMD2* mutations but exhibiting normal LPs indicate that the diminished LP that is diagnostic for BMD is not the pathophysiological cause of vision loss in these individuals.

The authors are grateful to Tyson Kinnick, Ji-Eun Choi, and Anna Yocom for their assistance in characterizing *Vmd2* mutant mice, to Dr. Philippe Soriano for providing the PGKneolox2DTA vector, and to Dr. Sherry Ball (Cleveland VA Medical Center) for providing $\beta_1$ and $\beta_2$ mutant mice.

Work in the author's laboratories is made possible by grants from Phillip Morris USA and Phillip Morris International (A.D. Marmorstein), the National Institutes of Health (EY13160 and EY14898 to A.D. Marmorstein; EY13847 to L.Y. Marmorstein; EY14465 and EY15638 to N.S. Peachey; EY12354 to R.G. Gregg), a Career Development Award from Research to Prevent blindness (L.Y. Marmorstein), the Medical Research Service, Department of Veterans Affairs (N.S. Peachey), DFG grant STR480/91-1 (O. Strauss), the ProRetina Foundation (R. Neussert), and an unrestricted grant from Research to Prevent Blindness to the Department of Ophthalmology and Vision Science at the University of Arizona.

Lawrence G. Palmer served as editor.

Submitted: 14 December 2005
Accepted: 30 March 2006

## REFERENCES

Allikmets, R., J.M. Seddon, P.S. Bernstein, A. Hutchinson, A. Atkinson, S. Sharma, B. Gerrard, W. Li, M.L. Metzker, C. Wadelius, et al. 1999. Evaluation of the Best disease gene in patients with age-related macular degeneration and other maculopathies. *Hum. Genet.* 104:449–453.

Bakall, B., L.Y. Marmorstein, G. Hoppe, N.S. Peachey, C. Wadelius, and A.D. Marmorstein. 2003. Expression and localization of bestrophin during normal mouse development. *Invest. Ophthalmol. Vis. Sci.* 44:3622–3628.

Ball, S.L., P.A. Powers, H.-S. Shin, C.W. Morgans, N.S. Peachey, and R.G. Gregg. 2002. Role of the $\beta_2$ subunit of voltage-dependent calcium channels in the retinal outer plexiform layer. *Invest. Ophthalmol. Vis. Sci.* 43:1595–1603.

Blair, N.P., M.F. Goldberg, G.A. Fishman, and T. Salzano. 1984. Autosomal dominant vitreoretinochoroidopathy (ADVIRC). *Br. J. Ophthalmol.* 68:2–9.

Bösl, M.R., V. Stein, C. Hubner, A.A. Zdebik, S.E. Jordt, A.K. Mukhopadhyay, M.S. Davidoff, A.F. Holstein, and T.J. Jentsch. 2001. Male germ cells and photoreceptors, both dependent on close cell-cell interactions, degenerate upon ClC-2 $Cl^-$ channel disruption. *EMBO J.* 20:1289–1299.

Burgess, D.L., J.M. Jones, M.H. Meisler, and J.L. Noebels. 1997. Mutation of the $Ca^{2+}$ channel β subunit gene *Cchb4* is associated with ataxia and seizures in the *lethargic* (*lh*) mouse. *Cell.* 88:385–392.

Burgess, D.L., G.H. Biddlecome, S.I. McDonough, M.E. Diaz, C.A. Zilinski, B.P. Bean, K.P. Campbell, and J.L. Noebels. 1999. β subunit reshuffling modifies N- and P/Q-type $Ca^{2+}$ channel subunit compositions in lethargic mouse brain. *Mol. Cell. Neurosci.* 13:293–311.

Cross, H.E., and L. Bard. 1974. Electro-oculography in Best's muscular dystrophy. *Am. J. Ophthalmol.* 77:46–50.

Deutman, A.F. 1969. Electro-oculography in families with vitelliform dystrophy of the fovea. *Br. J. Ophthalmol.* 81:305–316.

Escayg, A., M. De Waard, D.D. Lee, D. Bichet, P. Wolf, T. Mayer, J. Johnston, R. Baloh, T. Sander, and M.H. Meisler. 2000. Coding and noncoding variation of the human calcium-channel $\beta_4$-subunit gene *CACNB4* in patients with idiopathic generalized epilepsy and episodic ataxia. *Am. J. Hum. Genet.* 66:1531–1539.

Fischmeister, R., and H.C. Hartzell. 2005. Volume sensitivity of the bestrophin family of chloride channels. *J. Physiol.* 562:477–491.

Frangieh, G.T., W.R. Green, and S.L. Fine. 1982. A histopathologic study of Best's macular dystrophy. *Arch. Ophthalmol.* 100:1115–1121.

Gallemore, R.P., B.A. Hughes, and S.S. Miller. 1998. Light-induced responses of the retinal pigment epithelium. *In* The Retinal Pigment Epithelium. M.F. Marmor, T.J. Wolfensberger, editors. Oxford University Press, New York. 175–198.

Gallemore, R.P., and R.H. Steinberg. 1989. Effects of DIDS on the chick retinal pigment epithelium. II. Mechanism of the light peak and other responses originating at the basal membrane. *J. Neurosci.* 9:1977–1984.

Gass, D.J.M. 1997. Heredodystrophic disorders affecting the pigment epithelium and retina. *In* Stereoscopic atlas of macular diseases, diagnosis and treatment. Volume 1. D.J.M. Gass, editor. Mosby, St. Louis, MI. 303–313.

G odel, V., G. Chaine, L. Regenbogen, and G. Coscas. 1986. Best's vitelliform macular dystrophy. *Acta Ophthalmol. Suppl.* 175:1–31.

Gregg, R.G., A. Messing, C. Strube, M. Beurg, R. Moss, M. Behan, M. Sukhareva, S. Haynes, J.A. Powell, R. Coronado, and P.A. Powers. 1996. Absence of the $\beta_1$ subunit (cchb1) of the skeletal muscle dihydropyridine receptor alters expression of the $\alpha_1$ subunit and eliminates excitation-contraction coupling. *Proc. Natl. Acad. Sci. USA.* 93:13961–13966.

Griff, E.R., and R.H. Steinberg. 1984. Changes in apical [$K^+$] produce delayed basal membrane responses of the retinal pigment epithelium in the gecko. *J. Gen. Physiol.* 83:193–211.

Grynkiewicz, G., M. Poenie, and R.Y. Tsien. 1985. A new generation of $Ca^{2+}$ indicators with greatly improved fluorescence properties. *J. Biol. Chem.* 260:3440–3450.

Han, D.P., and M.F. Lewandowski. 1992. Electro-oculography in autosomal dominant vitreoretinochoroidopathy. *Arch. Ophthalmol.* 110:1563–1567.

Hartzell, C., I. Putzier, and J. Arreola. 2005. Calcium-activated chloride channels. *Annu. Rev. Physiol.* 67:719–758.

Kofuji, P., P. Ceelen, K.R. Zahs, L.W. Surbeck, H.A. Lester, and E.A. Newman. 2000. Genetic inactivation of an inwardly rectifying potassium channel (Kir4.1 subunit) in mice: phenotypic impact in retina. *J. Neurosci.* 20:5733–5740.

Kramer, F., K. White, D. Pauleikhoff, A. Gehrig, L. Passmore, A. Rivera, G. Rudolph, U. Kellner, M. Andrassi, B. Lorenz, et al. 2000. Mutations in the *VMD2* gene are associated with juvenile-onset vitelliform macular dystrophy (Best disease) and adult vitelliform macular dystrophy but not age-related macular degeneration. *Eur. J. Hum. Genet.* 8:286–292.

Linsenmeier, R.A., and R.H. Steinberg. 1983. A light-evoked interaction of apical and basal membranes of retinal pigment epithelium: c-wave and light peak. *J. Neurophysiol.* 50:136–147.

Linsenmeier, R.A., and R.H. Steinberg. 1984. Delayed basal hyperpolarization of cat retinal pigment epithelium and its relation to the fast oscillation of the DC electroretinogram. *J. Gen. Physiol.* 83:213–232.

Marmor, M.F. 1979. "Vitelliform" lesions in adults. *Ann. Ophthalmol.* 11:1705–1712.

Marmorstein, A.D., L.Y. Marmorstein, M. Rayborn, X. Wang, J.G. Hollyfield, and K. Petrukhin. 2000. Bestrophin, the product of the Best vitelliform macular dystrophy gene (VMD2), localizes to the basolateral plasma membrane of the retinal pigment epithelium. *Proc. Natl. Acad. Sci. USA.* 97:12758–12763.

Marmorstein, A.D., J.B. Stanton, J. Yocom, B. Bakall, M.T. Schiavone, C. Wadelius, L.Y. Marmorstein, and N.S. Peachey. 2004. A model of best vitelliform macular dystrophy in rats. *Invest. Ophthalmol. Vis. Sci.* 45:3733–3739.

Marquardt, A., H. Stohr, L.A. Passmore, F. Kramer, A. Rivera, and B.H. Weber. 1998. Mutations in a novel gene, VMD2, encoding a protein of unknown properties cause juvenile-onset vitelliform macular dystrophy (Best's disease). *Hum. Mol. Genet.* 7:1517–1525.

Mergler, S., and O. Strauss. 2002. Stimulation of L-type $Ca^{2+}$ channels by increase of intracellular $InsP_3$ in rat retinal pigment epithelial cells. *Exp. Eye Res.* 74:29–40.

Mitchell, C.H. 2001. Release of ATP by a human retinal pigment epithelial cell line: potential for autocrine stimulation through subretinal space. *J. Physiol.* 534:193–202.

Mullins, R.F., K.T. Oh, E. Heffron, G.S. Hageman, and E.M. Stone. 2005. Late development of vitelliform lesions and flecks in a patient with Best disease: clinicopathologic correlation. *Arch. Ophthalmol.* 123:1588–1594.

O'Gorman, S., W.A. Flaherty, G.A. Fishman, and E.L. Berson. 1988. Histopathologic findings in Best's vitelliform macular dystrophy. *Arch. Ophthalmol.* 106:1261–1268.

Peachey, N.S., J.B. Stanton, and A.D. Marmorstein. 2002. Response characteristics of the rat DC-electroretinogram. *Vis. Neurosci.* 19:693–701.

Peterson, W.M., C. Meggyesy, K. Yu, and S.S. Miller. 1997. Extracellular ATP activates calcium signaling, ion, and fluid transport in retinal pigment epithelium. *J. Neurosci.* 17:2324–2337.

Petrukhin, K., M.J. Koisti, B. Bakall, W. Li, G. Xie, T. Marknell, O. Sandgren, K. Forsman, G. Holmgren, S. Andreasson, et al. 1998. Identification of the gene responsible for Best macular dystrophy. *Nat. Genet.* 19:241–247.

Putney, J.W., Jr., L.M. Broad, F.J. Braun, J.P. Lievremont, and G.S. Bird. 2001. Mechanisms of capacitative calcium entry. *J. Cell Sci.* 114:2223–2229.

Qu, Z., and C. Hartzell. 2004. Determinants of anion permeation in the second transmembrane domain of the mouse bestrophin-2 chloride channel. *J. Gen. Physiol.* 124:371–382.

Qu, Z., R.W. Wei, W. Mann, and H.C. Hartzell. 2003. Two bestrophins cloned from *Xenopus laevis* oocytes express $Ca^{2+}$-activated $Cl^-$ currents. *J. Biol. Chem.* 278:49563–49572.

Qu, Z., R. Fischmeister, and C. Hartzell. 2004. Mouse bestrophin-2 is a bona fide $Cl^-$ channel: identification of a residue important in anion binding and conduction. *J. Gen. Physiol.* 123:327–340.

Reigada, D., and C.H. Mitchell. 2005. Release of ATP from retinal pigment epithelial cells involves both CFTR and vesicular transport. *Am. J. Physiol. Cell Physiol.* 288:C132–C140.

Robson, J.G., and L.J. Frishman. 1995. Response linearity and kinetics of the cat retina: the bipolar cell component of the dark-adapted electroretinogram. *Vis. Neurosci.* 12:837–850.

Robson, J.G., and L.J. Frishman. 1998. Dissecting the dark-adapted electroretinogram. *Doc. Ophthalmol.* 95:187–215.

Robson, J.G., S.M. Saszik, J. Ahmed, and L.J. Frishman. 2003. Rod and cone contributions to the a-wave of the electroretinogram of the macaque. *J. Physiol.* 547:509–530.

Rosenthal, R., B. Bakall, T. Kinnick, N. Peachey, S. Wimmers, C. Wadelius, A. Marmorstein, and O. Strauss. 2006. Expression of bestrophin-1, the product of the *VMD2* gene, modulates voltage-dependent $Ca^{2+}$ channels in retinal pigment epithelial cells. *FASEB J.* 20:178–180.

Seddon, J.M., M.A. Afshari, S. Sharma, P.S. Bernstein, S. Chong, A. Hutchinson, K. Petrukhin, and R. Allikmets. 2001. Assessment of mutations in the Best macular dystrophy (VMD2) gene in patients with adult-onset foveomacular vitelliform dystrophy, age-related maculopathy, and bull's-eye maculopathy. *Ophthalmology.* 108:2060–2067.

Stanton, J.B., A.F.X. Goldberg, G. Hoppe, L.Y. Marmorstein, and A.D. Marmorstein. 2006. Hydrodynamic properties of porcine bestrophin-1 in Triton X-100. *Biochim. Biophys. Acta.* 10.1016/j.bbamem.2006.01.024

Steinberg, R.H., R.A. Linsenmeier, and E.R. Griff. 1985. Retinal pigment epithelial cell contributions to the electroretinogram and electrooculogram. *In* Progress in Retinal Research. Volume 4. N.N. Osborne, G.J. Chader, editors. Pergamon Press, Oxford. 33–66.

Sun, H., T. Tsunenari, K.W. Yau, and J. Nathans. 2002. The vitelliform macular dystrophy protein defines a new family of chloride channels. *Proc. Natl. Acad. Sci. USA.* 99:4008–4013.

Tsunenari, T., H. Sun, J. Williams, H. Cahill, P. Smallwood, K.W. Yau, and J. Nathans. 2003. Structure-function analysis of the bestrophin family of anion channels. *J. Biol. Chem.* 278:41114–41125.

Ueda, Y., and R.H. Steinberg. 1994. Chloride currents in freshly isolated rat retinal pigment epithelial cells. *Exp. Eye Res.* 58:331–342.

Weingeist, T.A., J.L. Kobrin, and R.C. Watzke. 1982. Histopathology of Best's macular dystrophy. *Arch. Ophthalmol.* 100:1108–1114.

Wersto, R.P., E.R. Rosenthal, R.G. Crystal, and K.R. Spring. 1996. Uptake of fluorescent dyes associated with the functional expression of the cystic fibrosis transmembrane conductance regulator in epithelial cells. *Proc. Natl. Acad. Sci. USA.* 93:1167–1172.

White, K., A. Marquardt, and B.H. Weber. 2000. VMD2 mutations in vitelliform macular dystrophy (Best disease) and other maculopathies. *Hum. Mutat.* 15:301–308.

Wu, J., A.D. Marmorstein, P. Kofuji, and N.S. Peachey. 2004a. Contribution of Kir4.1 to the mouse electroretinogram. *Mol. Vis.* 10:650–654.

Wu, J., N.S. Peachey, and A.D. Marmorstein. 2004b. Light-evoked responses of the mouse retinal pigment epithelium. *J. Neurophysiol.* 91:1134–1142.

Wu, J., A.D. Marmorstein, and N.S. Peachey. 2006. Functional abnormalities in the retinal pigment epithelium of CFTR-mutant mice. *Exp. Eye Res.* In press.

Yardley, J., B.P. Leroy, N. Hart-Holden, B.A. Lafaut, B. Loeys, L.M. Messiaen, R. Perveen, M.A. Reddy, S.S. Bhattacharya, E. Traboulsi, et al. 2004. Mutations of VMD2 splicing regulators cause nanophthalmos and autosomal dominant vitreoretinochoroidopathy (ADVIRC). *Invest. Ophthalmol. Vis. Sci.* 45:3683–3689.

Zhou, L., C.R. Dey, S.E. Wert, M.D. DuVall, R.A. Frizzell, and J.A. Whitsett. 1994. Correction of lethal intestinal defect in a mouse model of cystic fibrosis by human CFTR. *Science.* 266:1705–1708.